



## Nuclear Energy Levels Scheme of Sc46 by Using FPD6 and KB3G Interaction

Hasan Ali Kadhim<sup>1\*</sup> and Firas Zuhair Majeed<sup>2</sup>

<sup>1,2</sup>Department of Physics College of Sciences, University of Baghdad, Baghdad, Iraq.

\*Corresponding author.

Received:30 May 2023

Accepted:3 July 2023

Published:20 July 2024

[doi.org/10.30526/37.3.3514](https://doi.org/10.30526/37.3.3514)

### Abstract

Nuclear energy levels in  $^{46}\text{Sc}$  with modest occupancy of the fp-LS shell have been studied within shell model calculations. The interactions used to determine the nuclear energy levels are FPD6, KB3G, and FPY using the fp shell and d3f7cospn for 1d3/21f7/2 model space. Results are compared with each other, and with the existing experimental data, there is clear agreement with some results. Aside from the excellent agreements in the replicated values of energy levels scheme, using model space interactions is the best-fitted two-body matrix element in the fp shell model space. Particularly below 3MeV, the overall estimation of the replicated data is excellent. The wave vectors and analysis are represented in the so-called diagrammatic notation, and all inscriptions are provided in this style. A single particle vector is generated by utilizing the oscillator's potential and considering  $^{40}\text{Ca}$  as the core for the fp shell model space and  $^{32}\text{S}$  as the inactive core for the d3f7 model space. Results are obtained for all examined nuclei using the OXFORD BEUNES AIRES SHELL MODEL CODE.

**Keywords:** Energy levels - Sc46 - Fp shell - OXBASH Code - Fpd6.

### 1. Introduction

The features and internal structure of the nucleus have been the subject of much research. There is no all-encompassing theory that can adequately describe the operations, characteristics, and structures of nuclei[1]. The shell theory provides several benefits and features, including model independence, the applicability of the practical N-N potential, and a broad variety of nuclei, in addition to the conventional Hamiltonian related to various kinds of eigenvectors. Obtaining all observable nuclei follows naturally from the shell theory; hence, it is still applicable today[1]. Using the LS shell (1f7/2 1f5/2 2p3/2 2p1/2) as a reference, they determined the excitation energies, binding energies, and spectral factors necessary to generate the effective N-N matrix elements [2]. Using the nuclear shell model, the energy levels of different Cu and Ga nuclei were analyzed. An inert  $^{56}\text{Ni}$  nucleus was used as a model in the theoretical application, with pf single particle orbitals



serving as the model space. Using the  $f5pvh$  nucleon-nucleon interaction, the effective interactions between two nucleons were computed. Space-time dynamics have been modeled using orbits with radii of  $f5/2$ ,  $p3/2$ , and  $p1/2$  [3]. The goal of this study is to provide a method for efficiently and correctly disseminating computational results for shell models, with an emphasis on  $fp$ -shell. These estimations were based on the evaluation of Hamiltonian eigenvalues, which are compatible with positive parity of energy levels up to (10MeV) for most Ca isotopes, and the Hamiltonian eigenvectors transition strength probability, and inelastic electron-nucleus scattering. The Hamiltonian has proven to be helpful in the experimental settings we've used so far. The experimental data were used to propose a new nuclear level. To do the calculations the OXBASH, code [4] is utilized.

Calculations using the interaction of GXFP1 in the  $fp$  model space by adopting the single-particle wave functions of the harmonic oscillator. All of the isotopes involved have valence nucleons moving in  $1f7/2$ ,  $2p3/2$ ,  $1f5/2$ , and  $2p1/2$  orbitals, while the  $^{40}Ca$  nucleus is thought to have a stable nucleophile in the  $fp$ -form. The consequences of core polarization may be derived using microscopic theory in the case of first-order core polarization. To account for core polarization, the quadrupole and magnetic moments were calculated using the effective charge and effective  $g$  factors, respectively [5].

Three isotopes,  $^{46-45}Ca$ ,  $^{46-45}Ti$  and  $^{46-45}Sc$ , had their potential energies calculated. They conducted computations in the  $f7$ -shell region while accounting for the spin-parity of the valence nucleons using the shell model code OXBASH for Windows and the effective interactions,  $f748pn$ . It was shown that the energy level values tend to converge around the usable norm [6]. The nuclear energy levels of the even-even  $Ca$  isotopes were calculated using the nuclear shell model and the KShell computer code. This software allows us to do nuclear shell-model calculations using the M-scheme representation. The very potent  $^{40}Ca$  isotope was employed as the backbone of the calculations. It is possible for neutrons to simulate orbits at  $0f7/2$ ,  $1p3/2$ ,  $0f5/2$ , and  $1p1/2$  in their model space. Nuclear spin, parity, and energy have all been determined for excited Ca isotopes [7]. Using the interacting boson model-1 (IBM-1), they collected data on the A50 mass region of even-even Ti isotopes and examined their collective properties. In this study, the energy levels and rates of electromagnetic transitions for the isotopes  $^{44-48}Ti$  and  $^{52-60}Ti$  are determined. The IBM-1 models did not include the isotope  $^{50}Ti$  since its neutron count is 28 and 28 is considered the "magic number." The energy ratios were originally examined by comparing the normal values of the U(5), SU(3), and O(6) dynamical symmetries and the E(5), X(5) critical point symmetries. Based on the observable properties of the isotopes in the issue, a subsequent model Hamiltonian was constructed. Using the parameters of the fitted Hamiltonian, the lowest energy levels of all the Ti isotopes were calculated [8].

The shell model based on large-scale unconstrained  $fp$ -model space has been used to determine low-lying energy levels and Gamow-Teller B(GT) transition strengths for the transitions ( $^{42}Ca$   $^{42}Sc$ ,  $^{42}Ca$   $^{42}Ti$ ,  $^{45}Sc$   $^{45}Ca$ ,  $^{45}Sc$   $^{45}Ti$ ,  $^{45}V$   $^{45}Ti$ ). The intensities of the Gamow-Teller B(GT) transition were computed and compared to experimental data on concentrations. The low-lying energy levels of the studied nuclei were accurately reproduced. For several of the nuclei examined, the spin and parity of previously unconfirmed energy levels had been verified [9]. Energy levels and the

probability of electric transition B(E2) in the fp shell of the  $^{60}\text{Ni}$  and  $^{60}\text{Fe}$  nucleus with the effective interactions f5pvh, gx1, and kb3 were calculated using OXBASH. OXBASH is a computer application for calculating nuclear installations using a shell mode [10]. They computed the energy levels and the reduced electric quadrupole transition probability B(E2) for the 50Fe isotope using the OXBASH algorithm and the F754 and F7mbz effective interactions. There are six protons and four neutrons in the shell around the  $^{40}\text{Ca}$  nucleus of the  $^{50}\text{Fe}$  isotope. All of these isotopes had identical total angular momentum and ground state parity, and although this produced new energy levels, none of them was currently useful [11]. Within shell model calculations had been interested in nuclear energy levels; total angular momenta and even-even parity for nucleons that are presented outside closed and no core for the elements ( $^{42}\text{Ca}$ ,  $^{44}\text{Ca}$ ,  $^{46}\text{Ca}$ , and  $^{48}\text{Ca}$ ) that filled fp-shells (1f7/2,1f5/2,2p3/2,2p1/2). The atomic energy distribution over the periodic table ( $^{42}\text{Ca}$ ,  $^{44}\text{Ca}$ ,  $^{46}\text{Ca}$ , and  $^{48}\text{Ca}$ ) were determined via a total of four interactions. We compare the findings from the FPD6, GXPF1, and KB3G interactions with the GOGNY-P2 (fp, fpg, and fpgd model space) interactions and find some agreement.

The frozen orbitals and limited occupations method [12] were developed for use in full-space computations where the GOGNY-P2 interaction was used as the effective full-space two-body interaction. A nuclear shell model with ca as an inert core and FPD6, HW, and FPY as model space effective interactions was used to examine  $^{44}\text{Sc}$  [13] and  $^{44}\text{Ca}$  [14] nuclear energy levels, and the replicated results were compared to experimental data. In this investigation, they employed the OXBASH method to produce model space wave vectors and to receive the equivalent model space effective interaction. By considering the single-particle potential (harmonic oscillator) and the elastic magnetic electron scattering form factors, they established a model space factor for  $^{41}\text{Ca}$  using F7MBZ, with  $^{40}\text{Ca}$  as the inert core. Then, the Ca quadrupole moments (41, 43, 45, and 47) are calculated using the shell model [16], and the nuclear shell theory is applied to the entire system [15]. The theoretical level schemes of the selected nuclear states provide the basis for our FP-space model computations of different effective interactions. Spins and association energies that are common in GX1A, KB3G, FPD6, and GX1A are present in several experimentally observed levels in  $^{52}\text{Ca}$ . Spin spectra  $^{52-54}\text{Ca}$  and  $^{56-58}\text{Ca}$  were produced for efficient interactions [17]. Some physical properties, like the electromagnetic properties' effects on the nuclear structure of certain, cobalt (Co) isotopes with mass numbers  $A = 56-60$ , have been analyzed. These properties include elastic longitudinal form factors, electric quadrupole moments, and magnetic dipole moments. All GXFP1 interaction calculations are performed in the fp model space, using the harmonic oscillator's single-particle wave functions [18]. The modified-surface one-boson exchange potential (MSOBEP) model developed for the sd-shell [19,20] was successfully applied to generate a six-parameter density-dependent interaction for the bottom section of the fp shell FPD6 [21-25]. Even when used in the contemporary GXPF1 method, the FPD6 interaction remains extremely effective. While FPD6 already has monopole interactions, including them may improve the effective SPE attained for [26]. Recently, the GXPF1 has made it possible to apply the entire Effective two-body matrix elements + group interaction (ETBME+G) technique to the fp shell interaction, which has

been done for all fp shell nuclei in the mass range (47-65)[27,28]. Future theoretical and experimental studies will focus on neutron-rich fp shell nuclei.

The aim of this research is to use the OXBASH code[29] to calculate the nuclear energy levels in  $^{46}\text{Sc}$  isotopes, with  $^{40}\text{Ca}$  serving as the inert core, FPD6, KB3G, and FBY representing the fp shell, FZMBZ representing the 1f7/2 subshell orbit, and D3F7COSPn representing the 1d3/2 1f7/2 model space.

## 2. Materails and Methods

A minimum of the total energy describes the ground state of the core and two additional nucleon systems. In general, the two extra nucleons are, therefore, in the lowest available single-particle orbit and are related to the total spin and isospin value for which  $E_r^{(1)}(\rho^2)$  assumes the smallest value. All other states indicate excited states, in which the two particles are connected to distinct values or one or both of the additional nucleons are excited into a separate single-particle orbit. As shown in eq. (1), the Hamiltonian of the core-plus-two-nucleon system may be divided into two parts [30]:

$$H = H_{core} + H_{12} \quad (1)$$

With [30]

$$H_{core} = \sum_{k=3}^A [T(k) + U(k)] + [\sum_{3=k<l}^A W(k, l) - \sum_{k=3}^A U(k)], \quad (2)$$

$$H_{12} = \sum_{k=1}^A [T(k) + U(k)] + [\sum_{k=1}^2 \sum_{l=3}^A W(k, l) + W(1, 2) - \sum_{k=1}^2 U(k)] \quad (3)$$

where  $H_{core}$  denotes the interaction of the core particles (designated by  $k=3, \dots, A$ ). Assuming the closed-shell core is inert, the contribution of H to total energy is constant. H denotes the contribution of the two extra particles. It is more precisely expressed as [30].

$$H_{12} = H_{12}^{(0)} + H_{12}^{(1)}. \quad (4)$$

where  $H_{12}^{(0)}$  Specifies the single-particle Hamiltonian given by [30]

$$H_{12}^{(0)} = [T(1) + U(1)] + [T(2) + U(2)] = H_{s.p.}(1) + H_{s.p.}(2) \quad (5)$$

A and  $H_{12}^{(1)}$  denotes the residual interaction and it is given by [30]

$$H_{12}^{(1)} = [\sum_{l=3}^A W(1, l) - U(1)] + [\sum_{l=3}^A W(2, l) - U(2)] + W(1, 2) \quad (6)$$

If we now take

$$U(k) = \sum_{l=3}^A W(k, l) \quad \text{For } k= 1, 2, \quad (7)$$

Only the two-particle term  $W(1,2)$  persists after the single-particle terms in the residual interaction  $H_{12}^{(1)}$  exactly vanish. In other words, it gives the residual interaction  $H_{12}^{(1)} = W(1, 2)$ , where  $W(1,2)$  lacks any words with a single particle.

According to the definition in equation (7), which sums up all of the core's particles, the single-particle states are defined by the core nucleus. The Hartree-Fock theory provides the general derivation of a self-consistent single-particle potential  $U$ . However, because the later approximation is so complicated, it won't be covered here. In the majority of shell-model computations, the assumption is made that the Saxon-Woods potential or the simple harmonic oscillator can be used to describe the single-particle potential.  $H_{12}^{(1)}$  is no longer equivalent to  $W(1, 2)$  in that scenario. It is now assumed that the residual interaction, as provided in eq. (6) may still be represented by a two-body interaction for such a simplified single-particle potential  $U$ . The remaining two-body interaction will now be defined by  $\sum_{i<j} V(i, j)$ . Consequently, one has [30] in the scenario of two active particles outside of a core:

$$H_{12}^{(1)} = V(1, 2) \quad (8)$$

For the entire Hamiltonian, the following can be written from equations (3), (4), (5), and (6):

$$H = H_{core} + H_{s.p.}(1) + H_{s.p.}(2) + V(1, 2). \quad (9)$$

The expected value [30] provides the binding energy of the nucleus when two particles outside the core are in orbit and related to spin and isospin :

$$E_{\Gamma}^b(A) = \left\langle \Phi_{\Gamma}^{(0)}(1, \dots, A) \left| H \right| \Phi_{\Gamma}^{(0)}(1, \dots, A) \right\rangle \quad (10)$$

As the anti-symmetrized product of the core wave function,  $\Phi_{00}(\text{core})$ , and the wave function  $\Phi_{\Gamma}^{(0)}(1, \dots, A)$  characterizing the additional two nucleons, the total Hamiltonian in the state  $\Phi_{\Gamma}^{(0)}(1, \dots, A)$  of the whole nucleus can be stated as follows [30]:

$$\Phi_{\Gamma}^{(0)}(1, \dots, A) = \mathcal{A}\{\Phi_{00}(\text{core})\Phi_{\Gamma}^{(0)}(1, 2)\}. \quad (11)$$

In the particles 3, ..., A and 1, 2, respectively, it is thought that the functions  $\Phi_{00}(\text{core})$  and  $\Phi_{\Gamma}^{(0)}(1, 2)$  are antisymmetric. By permuting particle coordinates and selecting suitable linear combinations, the antisymmetrizer  $\mathcal{A}$  must finish antisymmetrizing all particles. The right outcomes are likewise achieved using the more straightforward product function  $\Phi_{00}(\text{core})\Phi_{\Gamma}^{(0)}(1, 2)$  for the evaluation of the matrix element in equation (11). Since the whole Hamiltonian in equation (11) has been divided into terms that operate on particles 1, 2, or 3, A, one can derive the following from the orthonormality of the wave function:  $\Phi_{00}(\text{core})$  and  $\Phi_{\Gamma}^{(0)}(1, 2)$  [30]:

$$\Phi_{00}(\text{core}) \text{ and } \Phi_{\Gamma}^{(0)}(1, 2) \text{ [14] :}$$

$$\begin{aligned} \left\langle \Phi_{00}(\text{core})\Phi_r^{(0)}(1,2) \middle| H \middle| \Phi_{00}(\text{core})\Phi_r^{(0)}(1,2) \right\rangle &= \langle \Phi_{00}(\text{core}) | H_{\text{core}} | \Phi_{00}(\text{core}) \rangle + \\ \left\langle \Phi_r^{(0)}(1,2) \middle| H_{s.p.}(1) + H_{s.p.}(2) \middle| \Phi_r^{(0)}(1,2) \right\rangle &+ \left\langle \Phi_r^{(0)}(1,2) \middle| V(1,2) \middle| \Phi_r^{(0)}(1,2) \right\rangle \end{aligned} \quad (12)$$

The following Eqs. [20] provide a definition for the linked two-particle wave function  $\Phi_r(1,2)$  [14]:

$$\Phi_{JM}(j_a(1)j_b(2)) = \sum_{m_a m_b} \langle j_a m_a j_b m_b | JM \rangle \phi_{j_a m_a}(1) \phi_{j_b m_b}(2) \quad (13)$$

$$\begin{aligned} \Phi_{JM}^{\pm} &= \sqrt{\frac{1}{2}}(1 \pm P_{12})\Phi_{JM}(j_a(1)j_b(2)) = \sqrt{\frac{1}{2}}\{\Phi_{JM}(j_a(1)j_b(2)) \pm \\ &(-1)^{J-j_a-j_b}\Phi_{JM}(j_b(1)j_a(2))\} \end{aligned} \quad (14)$$

One may integrate out the coordinates of particle 2 for  $H_{s.p.}(1)$  matrix element evaluation in equation (12), and one can do the same for  $H_{s.p.}(2)$  matrix element evaluation in equation (12). The matrix elements for single-particle eigen states  $\rho$ , each reduce to expectation values of  $H_{s.p.}$  due to the orthonormality of the Clebsch-Gordan coefficients. It is discovered that Eq. (12) and Eq. (12) with the single-particle energies provided by [30] are identical.

$$2e_{\rho} = \left\langle \Phi_r^{(0)}(1,2) \middle| H_{s.p.}(1) + H_{s.p.}(2) \middle| \Phi_r^{(0)}(1,2) \right\rangle = \left\langle \rho^2 \middle| H_{12}^{(0)} \middle| \rho^2 \right\rangle_r \quad (15)$$

In [14], the residual interaction is provided :

$$E_r^{(1)}(\rho^2) = \left\langle \Phi_r^{(0)}(1,2) \middle| V(1,2) \middle| \Phi_r^{(0)}(1,2) \right\rangle = \langle \rho^2 | V(1,2) | \rho^2 \rangle_r \quad (16)$$

And the core's binding energy, as indicated by [14]

### 3. Results

For 46 sc, as explained in **Figure 1**, the system is pure, the experimental data has 30 values, the repeated data for the interaction (FPD6, FPY, KB36, F7MBZ, and d3F7COSPn) are good, and others have some problems. The interaction (FPD6 and KB3G) has good reproductions and minor differences from that of experimental data, and the ground state for this interaction is (4+), the first excited 6+, and the second is 3+, and the order of series is accorded with the KB3G interaction and F7MBZ up to 1Mev, but the differences between interactions are apparent. The best results are fit to KB3G, FPY, and F7MBZ, but the result of FPY is shifted upward, which reveals that the interaction in the same model space has changed actions in the value of the study below. The energy levels below  $E = 3$  meV are more interesting, while values above these ranges are difficult to duplicate because not all of the processes inside the nucleus are represented by the model used in our study. The d3F7cosPN interaction failed to 2 reproduce experimental data due to an apparent overlap in energy levels, which is less than 200 keV as shown in **Figure 2**, and it does not resemble previous interactions where it has a different model space from other interactions.

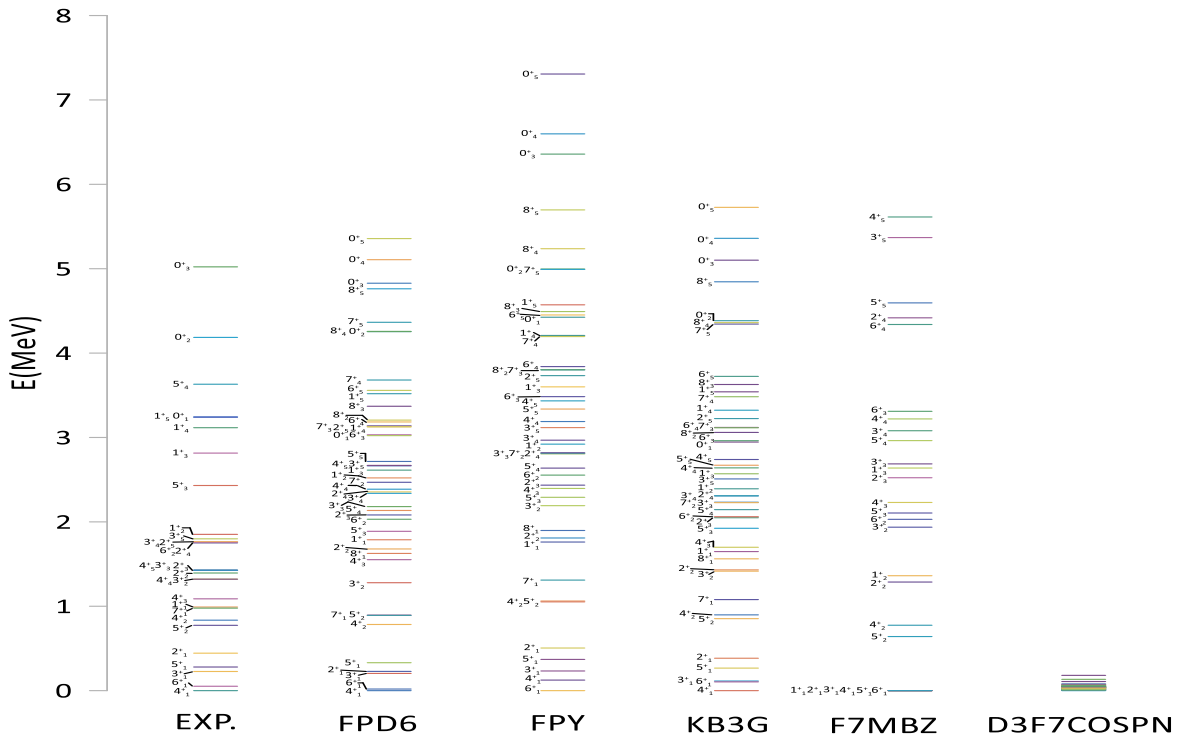


Figure 1. The energy levels system of  $^{46}\text{Sc}$  by using FPD6, FPY, KB3G, F7MBZ and D3F7COSP interactions with close core  $^{40}\text{Ca}$  and  $^{32}\text{S}$ , positive parity, ten order

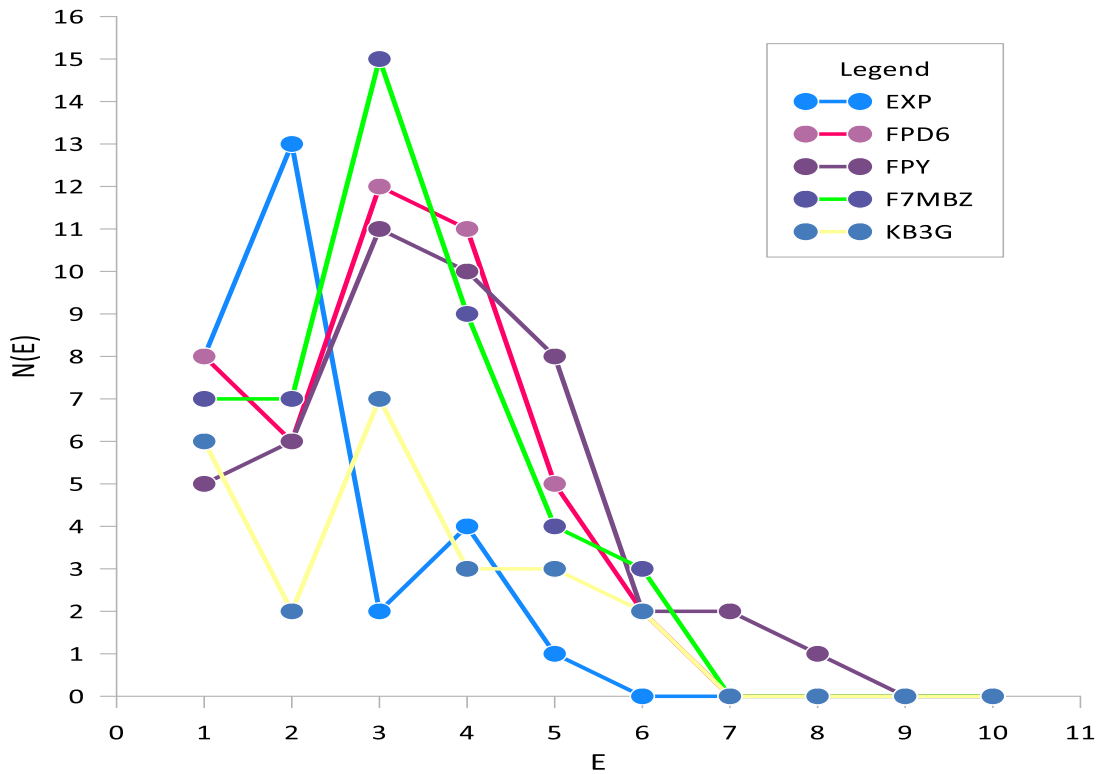


Figure 2. The density of states scheme of  $^{46}\text{Sc}$  per 1MeV

#### 4. Discussion

The terms of the two body matrix elements and the fitting parameter are anticipated by shell theory and residual interaction. Depending on the term constituting the interaction and the parameters under consideration, the intrusions either succeeded or failed to reproduce the experimental data. Some interactions are best fitted to the arrangement of (A), and their fitting parameters are normalized on (A-42) terms drawn from real (N-N) interactions and taking into consideration the channel of interaction (ST), where the meson particles represent the link between interacting nuclei. The density of energy levels, as shown in **Figure 2**, shows that the states are condensed in the range (2–3) MeV and reduced fast for all the interactions, and the value of the density of energy levels is different between the interactions. However, all of them indicate that the analyzers must be modified in order to obtain the energy level experimentally with a hyperfine structure.

#### 5. Conclusion

The quality and amount of recreated energy are both improved by Modern's effective interaction. In some model spaces and for some isotopes, the best choice of interaction is determined by the value of binding energies and separation energies for both neutrons and protons that can be reproduced by the chosen interaction, and then the interaction will succeed in model space in accordance with shell theory, which is still valid and confident in the reproduced theoretical results.

#### Acknowledgment

All thanks and appreciation to the College of Sciences, University of Baghdad for their valuable comments on this article, and thanks go to the journal's management and members.

#### Conflict of Interest

The authors declare that they have no conflicts of interest.

#### Funding

None.

#### References

1. Honma, M.; Otsuka, T.; Brown, B.A.; Minzusaki, T. Effective interaction for pf-shell nuclei. *Physical Review Journals*. **2002**, *65*, 12-23. <https://doi.org/10.1103/physrevc.65.061301>
2. Crannell, H.; Helm, R.; Kendall, H.; Oeser, J.; Yearian, M. Electron-Scattering Study of Nuclear Levels in Cobalt, Nickel, Lead, and Bismuth. *Physical Review Journals*. **1961**, *123*(3), 923. <https://doi.org/10.1103/physrev.123.923> .
3. Akkoyun, S.; Bayram, T.; Büyükata, M. Shell Model Calculations for some pf Shell Nuclei. *ALKU Journal of Science*. **2019**, *18*(2), 34-45.
4. Ali, A.M.; Khamees, A.A. Study of the Structure of Exotic 52,54,56,58Ca Isotopes Using OXBASH Code. *Iraqi Journal of Science*. **2019**, *60*(57), 55-67.



5. Hameed, B.S.; Rejah, B.K. Study the Nuclear Structure of Some Cobalt Isotopes. *Baghdad Science Journal*. **2022**, 19(6), 1566. <https://doi.org/10.21123/bsj.2022.753> .
6. Hasan, A.K.; Kareem, R.M. Calculation of Energy Levels and B(E2) for  $^{46-45}\text{Ca}$ ,  $^{46-45}\text{Sc}$  and  $^{46-45}\text{Ti}$  Using Shell Model Code OXBASH. *International Journal of Scientific and Research Publications*. **2019**, 9, 269. <https://doi.org/10.29322/ijsrp.9.08.2019.p9243>.
7. Akkoyun, S.; Ayhan, Y.; Bayram, T. Nuclear Shell Model Calculations for Ca Isotopes. *BEU Journal of Science*. **2020**, 9(3), 1102. <https://doi.org/10.17798/bitlisfen.665872>.
8. ŞAHİN, Y.; BÖYÜKATA, M.; Description of even-even Ti isotopes within IBM-1 model. *Cumhuriyet Science Journal*. **2021**, 42(1), 177. <https://doi.org/10.17776/cs.856118>
9. Obaid, S.M.; Majeed, F.A.; Mohammed, F.E. Nuclear structure and Gamow-teller b(gt) transition strengths for some selected fp-shell nuclei, *Karbala International Journal of Modern Science*. **2022**, 8, 522. <https://doi.org/10.17776/cs.856118> .
10. Hasan, A. K.; Salih, A.A. Calculation of Energy Levels and B(E2) for  $^{60}\text{Ni}$  and  $^{60}\text{Fe}$  Isotopes by Using Nuclear Shell Model. *National Qualification in Journalism*. **2022**, 20, 1050. <https://doi.org/10.14704/nq.2022.20.8.NQ44115> .
11. Hasan, A.K.; Salih, A.A. Energy Levels and B(E2) Calculation for  $^{50}\text{Fe}$  Isotope Using F754 and F7mbz Interactions. *National Qualification in Journalism*. **2022**, 20, 115. <https://doi.org/10.14704/nq.2022.20.5.nq22154> .
12. Majeed F.Z.; Mashaan, S.S. Energy Levels Calculation for Ca Isotopes Using Different Interactions. *Indian Journal of Natural Sciences*. **2018**, 9(50), 12-34.
13. Hassan, M.K.; Majeed, F.Z. FP shell effective interactions and nuclear shell structure of  $^{44}\text{Sc}$ . *East European journal of physics*. **2023**, 1, 89. [doi.org/10.26565/2312-4334-2023-1-07](https://doi.org/10.26565/2312-4334-2023-1-07) .
14. Hassan, M.K.; Majeed, F.Z. Nuclear energy levels in  $^{44}\text{Ca}$  using fpd6pn interaction. *East European journal of physics*. **2023**, 1, 69. [doi.org/10.26565/2312-4334-2023-1-10](https://doi.org/10.26565/2312-4334-2023-1-10).
15. Hussien, R.M.; Majeed, F.Z. The Effective M3Y Residual Interaction In  $^{41}\text{Ca}$  As a Nuclear Diffraction Grating of Electrons. *Baghdad Science Journal*. **2022**, 19(6), 1395. <https://doi.org/10.21123/bsj.2022.6776>.
16. Ali, A.H. Investigation of the Quadrupole Moment and Form Factors of Some Ca Isotopes. *Baghdad Science Journal*. **2020**, 17(2), 507. <https://doi.org/10.21123/bsj.2020.17.2.0502>
17. Ali, A.M.; Khamees, A.A. Study of the Structure of Exotic  $^{52,54,56,58}\text{Ca}$  Isotopes Using OXBASH Code. *Iraqi Journal of Science*. **2019**, 60, 60. <https://doi.org/10.24996/ij.2019.60.1.8m>
18. Hameed, B.S.; Rejah, B.K. Study the Nuclear Structure of Some Cobalt Isotopes. *Baghdad Science Journal*. **2022**, 19, 1566. <https://doi.org/10.21123/bsj.2022.7537>.
19. Schielke, S.; Speidel, K.H.; Kenn, O.; Leske, J.; Gemein, N.; Offer, M.; Sharon, Y.Y.; Zamick, L.; Gerber, J.; Maier-Komor, P. First measurement and shell model interpretation of the g factor of the 21+ state in self-conjugate radioactive  $^{44}\text{Ti}$ . *Physics Letters B*. **2003**, 567, 153–158. <https://doi.org/10.1016/j.physletb.2003.06.027>.
20. Schielke, S.; Hohn, D.; Speidel, K.H.; Kenn, O.; Leske, J.; Gemein, N.; Offer, M.; Gerber, J.; Maier-Komor, P.; Zell, O.; Sharon, Y.Y.; Zamick, L. Evidence for  $^{40}\text{Ca}$  core excitation from g

- factor and B(E2) measurements on the 21+ states of  $^{42,44}\text{Ca}$ . *Physics Letters B*. **2003**, 571, 29–35. <https://doi.org/10.1016/j.physletb.2003.08.015>.
21. Poves, A.; Sánchez-Solano, J.; Caurier, E.; Nowacki, F. Shell model study of the isobaric chains  $A=50$ ,  $A=51$  and  $A=52$ . *Nuclear Physics A*. **2001**, 694, 157–198. [https://doi.org/10.1016/s0375-9474\(01\)00967-8](https://doi.org/10.1016/s0375-9474(01)00967-8).
  22. Honma, M.; Otsuka, T.; Brown, B.A.; Mizusaki, T. Shell-model description of neutron-rich pf-shell nuclei with a new effective interaction GXPF 1. *The European Physical Journal A*. **2005**, 25, 499–502. <https://doi.org/10.1140/epjad/i2005-06-032-2>.
  23. Dinca, D.C.; Janssens, R.V.F.; Gade, A.; Bazin, D.; Broda, R.; Brown, B.A.; Campbell, C.M.; Carpenter, M.P.; Chowdhury, P.; Cook, J.M.; Deacon, A.N.; Fornal, B.; Freeman, S.J.; Glasmacher, T.; Honma, M.; Kondev, F.G.; Lecouey, J.-L.; Liddick, S.N.; Mantica, P.F.; Mueller, W.F.; Olliver, H.; Otsuka, T.; Terry, J.R.; Tomlin, B.A.; Yoneda, K. Reduced transition probabilities to the first 2+ state in  $^{52,54,56}\text{Ti}$  and development of shell closures at  $N=32,34$ . *Physical Review C*. **2005**, 71, 12. <https://doi.org/10.1103/physrevc.71.041302>.
  24. Bertsch, G.F.; Brown, B.A.; Sagawa, H. High-energy reaction cross sections of light nuclei. *Physical Review C*. **1989**, 39(2), 1154–1157. <https://doi.org/10.1103/physrevc.39.1154>.
  25. Dean, D.J.; Hjorth-Jensen, M. Pairing in nuclear systems: from neutron stars to finite nuclei. *Reviews of Modern Physics*. **2003**, 75, 607–656. <https://doi.org/10.1103/revmodphys.75.607>.
  26. Schmid, K.W.; Grümmner, F.; Faessler, A. Complex mean fields and unnatural parity pairing in the Hartree-Fock-Bogoliubov problem with symmetry-projection before the variation. *Annals of Physics*. **1987**, 180, 1–73. [https://doi.org/10.1016/0003-4916\(87\)90129-1](https://doi.org/10.1016/0003-4916(87)90129-1).
  27. Petrovici, A.; Schmid, K.W.; Faessler, A. Microscopic aspects of shape coexistence in  $^{72}\text{Kr}$  and  $^{74}\text{Kr}$ . *Nuclear Physics A*. **2000**, 665, 333–350. [https://doi.org/10.1016/s0375-9474\(99\)00811-8](https://doi.org/10.1016/s0375-9474(99)00811-8).
  28. Brown, B.A. Neutron Radii in Nuclei and the Neutron Equation of State. *Physical Review Letters*. **2000**, 85, 5296–5299. <https://doi.org/10.1103/physrevlett.85.5296>.
  29. Brown, B.A. OXBASH code, *Msunsl Report*. **1988**, 524(23), 34-56.
  30. Brussaard, P.J.; Glademans, P.W.M. Shell-model Applications in Nuclear Spectroscopy. *North-Holland Publishing Company, Amsterdam*. **1977**, 12(3), 66-76.